

Freezing of QCD coupling α_s affects the short distance static potential

A.M.Badalian¹, D.S.Kuzmenko²

*Institute of Theoretical and Experimental Physics,
Moscow, Russia*

Abstract

A striking contradiction between lattice short range static potential ($n_f = 0$) and standard perturbative potential, observed in Ref. [18], is investigated in the framework of the background perturbation theory. With the use of the background coupling $\tilde{\alpha}_B(r)$ which contains the only background parameter - mass m_B , fixed by fine structure fit in bottomonium, the lattice data are nicely explained without introduction of exotic short range linear potential with large "string tension" $\sigma^* \sim 1 \text{ GeV}^2$. A significant difference between $\tilde{\alpha}_B(r)$ and standard $\alpha_s(r)$ is found in the range $0.05 \text{ fm} \lesssim r \lesssim 0.15 \text{ fm}$, while at larger distances, $r > 0.3 \text{ fm}$ $\tilde{\alpha}_B(r)$ fast approaches the freezing value $\tilde{\alpha}_B(\infty)$. Some problems concerning the strong coupling properties at short and long distances are discussed and solutions are suggested.

1 Introduction

The property of freezing of the strong coupling running constant $\alpha_R(r)$ (or $\alpha_s(r)$ in different notations) at long distances is widely used in QCD phenomenology [1]-[6]. On the fundamental level this phenomenon has been studied in two different theoretical approaches [7]-[9]. In the case of the static potential the freezing of the vector coupling constant $\alpha_R(r)$ suggests that $\alpha_R(r)$ is approaching a constant $\alpha_{\text{fr}} \equiv \alpha_R(r \rightarrow \infty)$ at relatively long distances while at small r it manifests the property of asymptotic freedom. Both characteristic features of the static potential were widely used in hadron spectroscopy. However, it was realized that the asymptotic freedom behavior does not practically affect hadron spectra being important mostly for a wave function at the origin. On the contrary, the choice of $\alpha_R(r)$ as a constant at all distances, i.e. $\alpha_R(r) \cong \bar{\alpha}_R$, appears to be a reasonable approximation and gives rise to a good description of meson spectra both for heavy quarkonia [1, 10, 11] and for heavy-light mesons [12]. Also in lattice QCD this choice gives a good fit to lattice static potential at the distances above 0.2 fm.

Therefore the question arises why this simple approximation, $\alpha_R(r) \approx \bar{\alpha}_R$, works so well even in the case of bottomonium where the sizes of low-lying levels are not large, the characteristic radius $R_{\text{ch}} \lesssim 0.5 \text{ fm}$. To answer this question one needs to clarify another problem. Namely, to find out the precise freezing value of the vector constant in momentum and coordinate spaces, and to define the distances r where the difference between $\alpha_R(r)$ and α_{fr} is becoming inessential and therefore the approximation $\alpha_R(r) = \bar{\alpha}_R$ ($\bar{\alpha}_R \neq \alpha_{\text{fr}}$ in general case) gives a good description of hadron spectra and other physical characteristics.

¹e-mail: badalian@heron.itep.ru

²e-mail: kuzmenko@heron.itep.ru

This problem will be discussed in the present paper in the framework of background perturbation theory (BPTh) and it will be shown that the background coupling $\tilde{\alpha}_B(r)$ approaches its freezing value already at rather small distances $r > 0.4$ fm. Here it is worthwhile to remind that in most calculations in coordinate space the "average" value $\bar{\alpha}_R$ is usually taken in the range: $0.35 \lesssim \bar{\alpha}_R \lesssim 0.45$ while in momentum space larger critical values were used ($\alpha_{\text{cr}} \equiv \alpha_V(q=0)$), for example, in Ref. [3] $\alpha_{\text{cr}} = 0.60$ and for the Richardson potential $\alpha_{\text{cr}} = \frac{2\pi}{\beta_0} \approx 0.7$ ($n_f = 3$) [2, 13], i.e. the difference between $\alpha_{\text{cr}} \approx 0.6 \div 0.7$ in momentum space and $\bar{\alpha}_R \approx 0.40 \pm 0.05$ in coordinate space is essential. However, this difference was not confirmed by the analysis of the QCD coupling in background fields [14] where the vector coupling constants $\alpha_B(q)$ and $\tilde{\alpha}_B(r)$ were found to have the same asymptotic value:

$$\alpha_B(q=0) = \tilde{\alpha}_B(r \rightarrow \infty) = \alpha_{\text{fr}}. \quad (1)$$

This equality takes place also for the phenomenological coupling taken as a sum of Gaussians in Ref. [3].

In lattice measurements of the static potential at long distances the freezing phenomenon is also seen, however, existing lattice data have not clarified our knowledge about α_{fr} . As shown in Refs. [15], [16] lattice static potential at $r \geq 0.2$ fm can be parameterized with a good accuracy by Cornell potential with rather small $\bar{\alpha}_R$ (in lattice notation $\frac{4}{3}\bar{\alpha}_R = e$). In quenched approximation ($n_f = 0$) the fitted lattice values of $\bar{\alpha}_R \approx 0.20 \div 0.24$ ($e = 0.27 \div 0.32$) turned out to be small so that in some cases there appears a discontinuity of the vector coupling constant at the matching point, $r_{\text{mat}} \approx 0.2$ fm [5]. But if dynamical fermions are introduced in lattice QCD the fitted value of $\bar{\alpha}_R$ ($n_f = 2, 3$) was found to become larger: $\bar{\alpha}_R \cong 0.30$ ($e \cong 0.40$) [17] still being less than in phenomenological models.

Another problem concerns behavior of $\alpha_s(r)$ at short distances. The most interesting and unexpected results were obtained in lattice measurements of the static potential at short distances, $0.05 \text{ fm} \leq r \leq 0.15 \text{ fm}$ [18], where a large difference between lattice and two-loop (one-loop) perturbative potential was observed, yielding discrepancy about 100% at the point $r = 0.15$ fm. In Ref.[18] this large difference was parametrized by short distance linear term $\sigma^* r$ with the slope $\sigma^* \approx 1 \text{ GeV}^2$.

This effect will be explained in our paper. To this end the strong coupling constant in background fields $\tilde{\alpha}_B(r)$ will be calculated and the influence of the background mass m_B will be shown to become essential already at rather short distances. Resulting static potential $V_B(r)$ appears to have an additional effectively linear term in a good agreement with lattice data. In our calculations no fitting parameters are introduced: the value of the background mass $m_B = 1.0 \text{ GeV}$ is taken from fine structure analysis in bottomonium [11] while the QCD constant $\Lambda_{\overline{MS}}(n_f = 0)$ is considered as a well established number and taken from Ref.[19].

2 The strong coupling constant $\alpha_B(q)$ in background field theory

The perturbative static potential is used to define a vector coupling constant $\alpha_V(q)$:

$$V_P(q) = -4\pi C_F \frac{\alpha_V(q)}{q^2}, \quad (2)$$

where $q^2 \equiv \mathbf{q}^2$. Recently the renormalized $\alpha_V(q)$ was calculated in two-loop approximation [20, 21]. In coordinate space the static potential can be defined as the Fourier transform of $V_P(q)$,

$$V_P(r) = \int \frac{d\mathbf{q}}{(2\pi)^3} V_P(q) \exp(i\mathbf{q}\mathbf{r}), \quad (3)$$

which gives rise to the simple relation between the coupling constants:

$$\alpha_R(r) = \frac{2}{\pi} \int_0^\infty dq \frac{\sin qr}{q} \alpha_V(q), \quad (4)$$

if the following definition for the coupling in coordinate space $\alpha_R(r)$ is used,

$$V_P(r) = -C_F \frac{\alpha_R(r)}{r}. \quad (5)$$

However, the Fourier transform of the perturbative coupling $\alpha_V(q)$, Eq.(4), does not exist in a strict sense because of Landau pole singularity. To escape IR divergency the expansion of $\alpha_V(q)$ in the perturbative series at large q^2 is usually made [20, 21], but the resulting expansion is valid only at short distances.

Here we suggest to obtain the static potential in coordinate space with the use of the coupling in BPTh, where the vector coupling constant $\alpha_B(q)$ in momentum space is defined at all momenta and has no singularity for $q^2 > 0$ [7]. Then the potential in momentum space can be written as in Eq.(2),

$$V_B(q) = -C_F 4\pi \frac{\alpha_B(q)}{q^2}. \quad (6)$$

In Eq. (6) and below we consider the influence of background vacuum fields only on Coulomb-type interaction. In presence of background fields the QCD coupling is modified so that it depends on the combination $(q^2 + m_B^2)$ instead of q^2 as it is in standard perturbative theory [8]. The mass m_B is a background mass which is characteristic for a process considered. In two-loop approximation the running background coupling is

$$\alpha_B^{(2)}(q) = \alpha_B^{(1)}(q) \left\{ 1 - \frac{\beta_1}{\beta_0^2} \frac{\ln t_B}{t_B} \right\}, \quad (7)$$

where one-loop expression is given by

$$\alpha_B^{(1)}(q) = \frac{4\pi}{\beta_0 t_B}, \quad (8)$$

with

$$t_B = \ln \frac{q^2 + m_B^2}{\Lambda_V^2}. \quad (9)$$

The condition $m_B > \Lambda_V$ is assumed to be satisfied under the logarithm (9) to guarantee the absence of Landau pole; this condition is always valid for the numbers Λ_V and m_B used in our calculations (see the numbers in Eq.(25)).

In Eq.(7)

$$\beta_0 = 11 - \frac{2}{3}n_f; \beta_1 = 102 - \frac{38}{3}n_f. \quad (10)$$

First we discuss the most important properties of the background coupling $\alpha_B(q)$.

The background mass m_B is not an arbitrary parameter. It can be calculated in the framework of BPTth or in lattice QCD. As was shown in Ref. [22] the background mass m_B in the case of the static potential is defined by the difference of two-gluon and one-gluon hybrid excitations and can be extracted from the corresponding level differences of hybrids $c\bar{c}g, b\bar{b}g$. In Ref. [22] this mass m_B was evaluated to be $1.0 \div 1.2$ GeV. For other processes, like $e^+e^- \rightarrow$ hadrons, in general case the background mass m_B may be different [8]. The appearance of the mass m_B in Eq.(9) is similar to the case of QED where α has the mass of e^+e^- pair under logarithm.

It is of interest to notice that the analytical form of $\alpha_B(q)$ (7) coincides with that obtained in a picture when gluon is supposed to have an effective mass m_g inside gluon loop. Therefore in Refs. [23] $\alpha_s(q)$ was taken as a function of $(q^2 + 4m_g^2)$, i.e. the double effective gluon mass $2m_g$ plays a role of the background mass m_B (see a discussion in Ref. [4]).

In our calculations here the value of m_B will be fixed at $m_B = 1.0$ GeV taken from the fit to fine structure splittings in bottomonium [11].

At large momenta, $q^2 \gg m_B^2$, the background coupling goes over into the standard perturbative expression $\alpha_s(q)$. Therefore the QCD constants $\Lambda_{\overline{MS}}$ in PQCD and $\Lambda_{\overline{MS}}^B$ in BPTth must coincide, in any case it is true for the number of flavors $n_f = 5$. As can be directly calculated with the use of matching procedure they are also equal for $n_f = 4$.

The QCD constant Λ_V , entering the vector coupling $\alpha_V(q)$ in Eq. (2), can be expressed through $\Lambda_{\overline{MS}}(n_f)$ in \overline{MS} renormalization scheme [24]:

$$\Lambda_V^{(n_f)} = \Lambda_{\overline{MS}}^{(n_f)} \exp\left(\frac{a_1}{2\beta_0}\right), \quad (11)$$

with

$$a_1 = \frac{31}{3} - \frac{10}{9}n_f. \quad (12)$$

At present the values of $\Lambda_{\overline{MS}}^{(n_f)}$ are well established for the number of flavors $n_f = 5$: $\Lambda_{\overline{MS}}^{(5)} = 208 \pm_{23}^{25}$ MeV [25] and also for $n_f = 0$ due to analysis in lattice finite size technique [19]:

$$\Lambda_{\overline{MS}}^{(0)} = \frac{602(48)}{r_0}, \quad (13)$$

where r_0 denotes the Sommer scale. With the use of $r_0 \cong 0.5 \text{ fm} = 2.5 \text{ GeV}^{-1}$, taken in most lattice calculations [17, 18], one obtains

$$\Lambda_{\overline{MS}}^{(0)} = 237 \pm 19 \text{ MeV}, \quad (14)$$

then from Eq. (11) the QCD constant in the "vector" scheme is

$$\Lambda_V^{(0)} = 379 \pm 30 \text{ MeV}. \quad (15)$$

In three-loop approximation the background coupling

$$\alpha_B^{(3)}(q) = \alpha_B^{(1)}(q) \left\{ 1 - \frac{\beta_1}{\beta_0^2} \frac{\ln t_B}{t_B} + \frac{\beta_1^2}{\beta_0^4 t_B^2} \left[(\ln t_B)^2 - \ln t_B - 1 + \frac{\beta_2^V \beta_0}{\beta_1^2} \right] \right\}, \quad (16)$$

contains the term including β_2^V coefficient, which depends on a renormalization scheme and was calculated in Refs. [20, 21] (the coefficients β_0, β_1 do not depend on the renormalization

scheme); this coefficient

$$\beta_2^V = \beta_2^{\overline{\text{MS}}} - a_1\beta_1 + (a_2 - a_1^2)\beta_0. \quad (17)$$

Here a_1 is defined by Eq.(12) and

$$\beta_2^{\overline{\text{MS}}} = \frac{2857}{2} - \frac{5033}{18}n_f + \frac{325}{54}n_f^2, \quad (18)$$

$$\begin{aligned} a_2 = 9 \left(\frac{4343}{162} + 4\pi^2 - \frac{\pi^4}{4} + \frac{22}{3}\zeta(3) \right) + \frac{100}{81}n_f^2 - \\ - \frac{3}{2}n_f \left(\frac{1798}{81} + \frac{56}{3}\zeta(3) \right) - \frac{2}{3}n_f \left(\frac{55}{3} - 16\zeta(3) \right) \end{aligned} \quad (19)$$

In Eq.(19) $\zeta(3) = 1.202057$ denotes the Riemann ζ -function. In quenched approximation

$$a_2(n_f = 0) = 456,7488, \quad \beta_2^V(n_f = 0) = 4224,1817, \quad (20)$$

i.e. β_2^V coefficient turns out to be about 3 times larger than $\beta_2^{\overline{\text{MS}}}(n_f = 0) = \frac{2857}{2}$. As a result the third order correction in $\alpha_B^{(3)}(q)$ is much larger than in the same order expression of $\alpha_s^{\overline{\text{MS}}}(q)$. In what follows we shall consider only two-loop and one-loop couplings which do not depend on the renormalization scheme.

It is easy to find the first order correction to the perturbative coupling $\alpha_s(q)$ which comes from the expansion of $\alpha_B(q)$ in powers of m_B^2/q^2 . In two-loop approximation

$$\alpha_{\text{appr}}^{(2)}(\text{large } q) = \alpha_s^{(2)}(q) - \alpha_s^{(1)}(q) \frac{m_B^2}{q^2 \ln \frac{q^2}{\Lambda_V^2}}; \quad (21)$$

with

$$\alpha_s^{(2)}(q) = \alpha_s^{(1)}(q) \left(1 - \frac{\beta_1}{\beta_0^2} \frac{\ln y}{y} \right), \quad \alpha_s^{(1)}(q) = \frac{4\pi}{\beta_0 y}, \quad y = \ln \frac{q^2}{\Lambda_V^2}. \quad (22)$$

As seen from Eq.(21) a power-type correction appears in $\alpha_B(q)$ due to presence of the background mass, although this term contains also the factor $(\ln \frac{q^2}{\Lambda_V^2})^{-1}$ [26]. The approximate coupling $\alpha_{\text{appr}}^{(2)}(\text{large } q)$, Eq. (21), can be compared to the exact expression (7) for $\alpha_B^{(2)}(q)$ (see Table 1) where in our calculations the values of $m_B = 1.0$ GeV, $\Lambda_V^{(0)} = 385$ MeV ($n_f = 0$) were used. As seen from Table I at large momenta, $q \geq 4$ GeV, the background correction is less than 0.5%; at smaller momenta it grows and reaches 11% at $q = 2$ GeV and already 24% at $q = 1.5$ GeV; at momenta $q \rightarrow 1$ GeV the expansion (21) is not applicable anymore. Thus the approximation of the background coupling as a sum of the perturbative coupling $\alpha_s(q)$ plus the additional term given in Eq. (21) is valid only at $q \gtrsim 2.0$ GeV, while at smaller $q \lesssim 1.0$ GeV the exact expression (7) has to be used. Thus the representation of $\alpha_B(q)$ as a sum of perturbative and nonperturbative terms suggested in [6] is valid in our approach for $q \geq 2$ GeV.

Table 1 The comparison of the "exact" two-loop background coupling $\alpha_B^{(2)}(q)$ and the approximate coupling $\alpha_{\text{appr}}^{(2)}(\text{large } q)$ ($n_f = 0$, $\Lambda_V = 385$ MeV, $m_B = 1.0$ GeV).

q in GeV	1.5	2.0	2.5	3.0	3.5	4.0	5.0
$\alpha_B^{(2)}(q)$	0.221	0.215	0.202	0.190	0.181	0.173	0.1618
$\alpha_{\text{appr}}^{(2)}(q)$	0.256	0.227	0.207	0.193	0.183	0.174	0.1612

The behavior of $\alpha_B(q)$ in IR region. The freezing value of $\alpha_B^{(n)}(q)$ can be easily obtained from Eqs. (7)-(9), in particular, for two-loop coupling

$$\alpha_{\text{cr}}^{(2)} = \alpha_B^{(2)}(q^2 = 0) = \frac{4\pi}{\beta_0 t_0} \left\{ 1 - \frac{\beta_1}{\beta_0^2} \frac{\ln t_0}{t_0} \right\} \quad (23)$$

with

$$\alpha_{\text{cr}}^{(1)} = \frac{4\pi}{\beta_0 t_0}; \quad t_0 = t_B(q^2 = 0) = \ln \frac{m_B^2}{\Lambda_V^2}. \quad (24)$$

In what follows the notation $\alpha_{\text{cr}}^{(n)} = \alpha_B^{(n)}(q^2 = 0)$, as in potential models [3], is also used. The parameters m_B and Λ_V , present in t_B , are considered to be fixed: the value of m_B is taken from fine structure analysis of $2P$ - and $1P$ - states in bottomonium while the value $\Lambda_V^{(0)}(n_f = 0)$ is taken from lattice data and given by Eq.(14),

$$m_B = 1.0 \text{ GeV}, \quad \Lambda_V^{(0)}(n_f = 0) = 385 \text{ MeV}. \quad (25)$$

We suppose here that for $n_f = 3$ the constants $\Lambda_V^{(3)}$ and $\Lambda_V^{(0)}$ are approximately equal,

$$\Lambda_V(n_f = 3) \simeq \Lambda_V(n_f = 0) = 385 \pm 30 \text{ MeV} \quad (26)$$

Then the following critical values can be obtained from Eqs. (7),(15):

$$\alpha_{\text{cr}}^{(1)} = 0.598; \quad \alpha_{\text{cr}}^{(2)} = 0.428; \quad \alpha_{\text{cr}}^{(3)} = 0.805 \quad (n_f = 0) \quad (27)$$

$$\alpha_{\text{cr}}^{(1)} = 0.731; \quad \alpha_{\text{cr}}^{(2)} = 0.536; \quad \alpha_{\text{cr}}^{(3)} = 0.972 \quad (n_f = 3) \quad (28)$$

The third order coupling turns out to be about 90% ($n_f = 0$) and 80% ($n_f = 3$) larger than $\alpha_{\text{cr}}^{(2)}(n_f)$ because of large β_2^V coefficient (20). Then the question arises: what is the true critical value in momentum space? We see that the coupling $\alpha_B(3\text{-loop})$ contains the β_2^V coefficient dependent on renormalization scheme; second, the critical value $\alpha_{\text{cr}}^{(3)}(n_f = 3)$ appeared to be too large and not compatible with the numbers used in low-energy QCD phenomenology.

On the contrary the background coupling $\alpha_B^{(2)}(q)$ in two-loop approximation turns out to be rather close to the phenomenological $\alpha_{\text{ph}}(q)$ which is successfully used in hadron spectroscopy. For comparison $\alpha_{\text{ph}}(q)$ will be taken from the well-known paper of Godfrey and Isgur [3]:

$$\alpha_{\text{GI}} = 0.25 \exp(-q^2) + 0.15 \exp(-0.1q^2) + 0.20 \exp(-0.001q^2) \quad (29)$$

with q in GeV and $\alpha_{\text{cr}} = 0.60$.

In Fig.1 this phenomenological coupling is compared to the background coupling $\alpha_B^{(2)}(q)$ for $n_f = 3$. Here, as in Eq.(26), it is supposed that $\Lambda_V(n_f = 3) \cong \Lambda_V(n_f = 0)$ and for $\Lambda_V(n_f = 3)$ two values, are taken:

$$(A) \quad \Lambda_V(n_f = 3) = 385 \text{ MeV}$$

$$(B) \quad \Lambda_V(n_f = 3) = 410 \text{ MeV}. \quad (30)$$

These values of $\Lambda_V^{(3)}$ do not contradict those which are commonly used in $\overline{\text{MS}}$ renormalization scheme, and give rise to $\alpha_s(M_Z) = 0.118 \pm 0.001$. The connection between $\Lambda_{\overline{\text{MS}}}^{(n_f)}$ and $\Lambda_V^{(n_f)}$ is given by Eq.(11).

In Fig.1 the couplings $\alpha_{\text{GI}}(q)$ (solid line), $\alpha_B^{(2)}(q)$ in two-loop approximation with $\Lambda_V = 385$ MeV (dashed line), and $\alpha_B^{(2)}(q)$ with $\Lambda_V = 410$ MeV (dash-dotted line) and $m_B = 1.0$ GeV are shown. At the momentum $q = \bar{m}_c = 1.3$ GeV (\bar{m}_c is the running mass of c quark) the matching of the couplings was done with the following result for the QCD constant: $\Lambda_V(n_f = 4) = 0.325$ MeV in the case *A* and $\Lambda_V(n_f = 4) = 351$ MeV in the case *B*. As is seen from Fig.1 the background coupling $\alpha_B^{(2)}(q)$ in the case *B* (and to some extent in the case *A*) appears to be very close to the phenomenological coupling $\alpha_{\text{GI}}(q)$; the difference between them is less than 5% at small $q \lesssim 1.3$ GeV and less than 2% in the range $1.3 \leq q \leq 4$ GeV. So one can expect that with the use of the background coupling as good description of low-energy experimental data can be obtained as in Ref. [3] with the use of the phenomenological coupling. From here our estimate of the freezing value is about $0.53 \div 0.60$, and it is interesting to look at the expansion of the background coupling $\alpha_B(q)$ near the freezing point $q = 0$:

$$\alpha_{\text{appr}}^{(2)}(\text{small } q) = \alpha_{\text{cr}}^{(2)} - \alpha_{\text{cr}}^{(1)} \frac{q^2}{m_B^2 \ln \frac{m_B^2}{\Lambda_V^2}}, \quad (31)$$

where $\alpha_{\text{cr}}^{(2)}, \alpha_{\text{cr}}^{(1)}$ are the fixed numbers defined by m_B and Λ_V (see Eqs. (23), (24)). This approximation appears to be valid only in very narrow range of small momenta q , $0 \leq q \leq 0.4$ GeV, where the difference between $\alpha_B^{(2)}(q)$ and $\alpha_{\text{appr}}^{(2)}(\text{small } q)$ is less than 5%; but it already reaches 22% at $q = 1.0$ GeV.

Heavy-quark initiated jets can be successfully described at small momenta if the following assumption is made about an effective coupling constant $\alpha_{\text{eff}}(q)$ in infrared region [6]:

$$J_2(\text{fit}) = (2 \text{ GeV})^{-1} \int_0^{2 \text{ GeV}} dq \frac{\alpha_s^{\text{eff}}(q)}{\pi} = 0.18 \pm 0.01(\text{exp}) \pm 0.02(\text{th}). \quad (32)$$

As was shown in Ref.[6] this number does not depend on the form of $\alpha_{\text{eff}}(q)$ assumed in the fit. Our calculations of the integral (32) with the background coupling $\alpha_B^{(2)}(q)$ from Eq.(7) with $n_f = 3, \Lambda_V = 410$ MeV, $m_B = 1.0$ GeV give

$$J_2(\alpha_B) = (2 \text{ GeV})^{-1} \int_0^{2 \text{ GeV}} \frac{dq}{\pi} \alpha_B^{(2)}(q) = 0.134 \quad (33)$$

i.e. this number is by 26% smaller than $J_2(\text{fit})$ in Eq.(32). The same integral calculated with the phenomenological constant $\alpha_{\text{GI}}(q)$ (29) is also by 22% smaller than $J_2(\text{fit})$ (the central value):

$$J_2(\alpha_{\text{GI}}) = 0.14 \quad (34)$$

and very close to our number (33). One should notice here that the large number (32) in Ref.[6] could be connected with the large fitted value of $\alpha_s^{\overline{\text{MS}}}(M_Z) = 0.125 \pm 0.003(\text{exp}) = 0.004(\text{th})$, used in this Ref., while now the average $\alpha_s^{\overline{\text{MS}}}(M_Z) = 0.118 \pm 0.001$ is accepted [25].

In conclusion we give our predictions about the freezing values in momentum space:

$$\begin{aligned} \alpha_{\text{cr}}^{(1)} &= 0.598, \quad \alpha_{\text{cr}}^{(2)} = 0.428 \quad (n_f = 0, \quad \Lambda_V^{(0)} = 385 \text{ MeV}), \\ \alpha_{\text{cr}}^{(1)} &= 0.731, \quad \alpha_{\text{cr}}^{(2)} = 0.536 \quad (n_f = 3, \quad \Lambda_V^{(3)} = 385 \text{ MeV}), \\ \alpha_{\text{cr}}^{(1)} &= 0.783, \quad \alpha_{\text{cr}}^{(2)} = 0.582 \quad (n_f = 3, \quad \Lambda_V^{(0)} = 410 \text{ MeV}) \end{aligned} \quad (35)$$

3 The background coupling $\tilde{\alpha}_B(r)$ in coordinate space

From the explicit expressions of $\alpha_B^{(n)}(q)$ it is evident that the vector coupling $\alpha_B^{(n)}(q)$ is well defined at all momenta q^2 if the condition $m_B > \Lambda_V$ is satisfied. Therefore the Fourier transform can be used to define the static potential in coordinate space over all distances:

$$V_B(r) \equiv -C_F \frac{\tilde{\alpha}_B(r)}{r} = -C_F 4\pi \int \frac{\alpha_B(q)}{q^2} e^{i\mathbf{q}\mathbf{r}} \frac{d\mathbf{q}}{(2\pi)^3} \quad (36)$$

From here the relation similar to Eq.(4) follows:

$$\tilde{\alpha}_B(r) = \frac{2}{\pi} \int_0^\infty dq \frac{\sin qr}{q} \alpha_B(q) = \frac{2}{\pi} \int_0^\infty dx \frac{\sin x}{x} \alpha_B(x/r), \quad (37)$$

where now the background coupling $\alpha_B(x)$ depends on the variable

$$t_B(x) = \ln \frac{x^2 + m_B^2 r^2}{\Lambda_V^2 r^2} \quad (38)$$

This integral (37) cannot be taken analytically even in one-loop approximation and was calculated numerically in n -loop approximations ($n = 1, 2$) with the use of the parameters (25). The behavior of background coupling $\tilde{\alpha}_B^{(2)}(r)$ and $\tilde{\alpha}_B^{(1)}(r)$ is shown in Fig.2 in the range $0 \leq r \leq 1.4$ fm.

From Fig.2 one can see that two-loop background coupling in coordinate space is approaching the freezing value at relatively short distances, $r \gtrsim 0.4$ fm, and the values of $\tilde{\alpha}_B^{(n)}(r)$ ($n = 1, 2$) at the Sommer scale $r_0 \approx 0.5$ fm are following,

$$\tilde{\alpha}_B^{(1)}(r_0 = 0.5 \text{ fm}) = 0.574; \quad \tilde{\alpha}_B^{(2)}(r_0 = 0.5 \text{ fm}) = 0.404 \quad (39)$$

It is of interest to notice that the two-loop coupling at the distance r_0 practically coincides with the number $\bar{\alpha}_R = 0.39$ widely used in Cornell potential [1], while the one-loop coupling is too large. This fact that two-loop background coupling is almost constant already at $r \gtrsim 0.4$ fm can be considered as an important argument in favour of the choice $\tilde{\alpha}_B(r) = \text{const}$ in low energy spectroscopy. In Fig.3 $\tilde{\alpha}_B^{(2)}(r)$ is shown for two different values of the background mass: $m_B = 1.0$ GeV (solid line) and $m_B = 1.1$ GeV (dashed line). As seen from Fig.3 the difference between them is becoming essential already at $r \approx 0.3$ fm, being about 10% over all distances $r > 0.3$ fm; their freezing values are $\alpha_{\text{fr}}^{(2)}(m_B = 1.0 \text{ GeV}) = 0.428$, $\alpha_{\text{fr}}^{(2)}(m_B = 1.1 \text{ GeV}) = 0.382$ (in both cases $\Lambda_V^{(0)} = 385$ MeV).

The freezing value in coordinate space turns out to be just the same as in momentum space, i.e. for $n_f = 3$ and $n_f = 0$ ($\Lambda_V = 385$ MeV) they are given by the numbers from Eq. (35). This property is true also for the phenomenological potential used in Ref.[3]:

$$\alpha_{\text{GI}}(q = 0) = \alpha_{\text{GI}}(r \rightarrow \infty) = 0.60, \quad (40)$$

since in coordinate space the coupling $\alpha_{\text{GI}}(r)$ corresponding to $\alpha_{\text{GI}}(q)$ in Eq. (29) is

$$\alpha_{\text{GI}}(r) = 0.25\Phi(2r) + 0.15\Phi(1.581r) + 0.20\Phi(15.811r), \quad (41)$$

where $\Phi(z)$ is the error function. Thus for three flavors the phenomenological value $\alpha_{\text{fr}} \approx 0.6$ was found to be a bit larger than our number $\alpha_{\text{fr}}^{(2)} = 0.54$ (see Eq. (35) for $n_f = 3$).

With $\tilde{\alpha}_B(r)$ calculated above we can compare the background potential $V_B(r)$ (37) to the lattice static potential from Ref.[18]. Here we are mostly interested in short range potential, in particular, in the influence of background mass m_B on its behavior. The properties of $\tilde{\alpha}_B(r)$ at small r will be considered in the next Section.

4 $\tilde{\alpha}_B(r)$ at short distances

Recently very precise lattice measurements of the static potential at short distances were presented [18]. Having these data one has a unique opportunity to compare theoretical predictions about the background coupling and the potential $V_B(r)$ with precise lattice data in quenched approximation. We remind that our calculations of $\tilde{\alpha}_B^{(n)}(r)$ ($n = 1, 2$) were done without any arbitrary parameter: $\Lambda_V^{(0)} = 385$ MeV ($n_f = 0$) was fixed from lattice data (Eq.(14)) and $m_B = 1.0$ GeV from the fine structure splitting of $1P$ and $2P$ states in bottomonium. In Fig.4 $\tilde{\alpha}_B^{(n)}(r)$ is compared to the perturbative running coupling $\alpha_s^{(2)}(r)$ at $r \leq 0.12$ fm, $\alpha_s^{(2)}(r)$ is given by the expression ($r\Lambda_R \ll 1$)

$$\alpha_s^{(2)}(r) = \alpha_s^{(1)}(r) \left\{ 1 - \frac{\beta_1}{\beta_0^2} \frac{\ln y_R}{y_R} \right\} \quad (42)$$

with

$$\alpha_s^{(1)}(r) = \frac{4\pi}{\beta_0 y_R}, \quad y_R = \ln \frac{1}{\Lambda_R^2 r^2}, \quad (43)$$

and the following prescription for the value of QCD constant $\Lambda_R(n_f)$ [24],[13]

$$\Lambda_R^{(n_f)} = \Lambda_V^{(n_f)} \exp \gamma_E \quad (44)$$

In Eq. (44) γ_E is the Euler constant ($\gamma_E = 0.5772157$), and in quenched approximation $\Lambda_V^{(0)}$ is given by the number (14), therefore for $n_f = 0$

$$\Lambda_R^{(0)} = 684 \pm 53 \text{ MeV} \quad (45)$$

In our calculations below we take the number

$$\Lambda_R^{(0)} = 686 \text{ MeV}, \quad (46)$$

which corresponds to $\Lambda_V^{(0)} = 385$ MeV according to the relation (44).

The numerical comparison of the "exact" background coupling $\tilde{\alpha}_B^{(2)}(r)$ ($\Lambda_V = 385$ MeV, $n_f = 0$) and the corresponding perturbative $\alpha_s^{(2)}(r)$ with $\Lambda_R^{(0)}$ from Eq. (46) is presented in Table II for the distances in the range

$$0.002 \text{ fm} \leq r \leq 0.15 \text{ fm}. \quad (47)$$

Table 2 The background coupling $\tilde{\alpha}_B^{(2)}(r)$ ($\Lambda_V^{(0)} = 385$ MeV, $m_B = 1.0$ GeV) compared to perturbative coupling $\alpha_s^{(2)}(r)$ with $\Lambda_R^{(0)} = 686$ MeV.

r in fm	$\tilde{\alpha}_B^{(2)}(r)$	$\alpha_s^{(2)}(r)$	r in fm	$\tilde{\alpha}_B^{(2)}(r)$	$\alpha_s^{(2)}(r)$
0.002	0.0964	0.0924	0.024	0.1757	0.1667
0.004	0.11095	0.10505	0.030	0.1880	0.1807
0.006	0.1216	0.1209	0.0355	0.1988	0.1943
0.008	0.1303	0.1221	0.041	0.2085	0.2079
0.012	0.1446	0.1352	0.049	0.2204	0.2264
0.016	0.1564	0.1465	0.057	0.2311	0.2455
0.020	0.1666	0.1569	0.063	0.2384	0.2605

One can see that the difference between these two couplings,

$$\Delta\alpha_B^{(2)}(r) = \tilde{\alpha}_B^{(2)}(r) - \alpha_s^{(2)}(r), \quad (n = 1, 2), \quad (48)$$

has several prominent features.

First, at very short distances, $r < 0.04$ fm, the correction $\Delta\alpha_B^{(2)}(r)$ is positive, i.e.

$$\tilde{\alpha}_B^{(2)}(r) > \alpha_s^{(2)}(r) \quad (r < 0.04 \text{ fm}), \quad (49)$$

and relatively small. It is about 6% at $r = 0.02$ fm and still remains $\sim 4\%$ at much smaller $r = 0.002$ fm so that $\tilde{\alpha}_B^{(2)}(r)$ approaches the perturbative running coupling $\alpha_s^{(2)}(r)$ rather slowly. In one-loop approximation this correction can be calculated analytically if one expands the logarithm $t_B^{-1}(x)$ under the integral (38) in powers of $\frac{\ln(x^2 + m_B^2 r^2)}{2\ln(\Lambda_V r)}$ assuming that $\ln(\Lambda_V r) \gg 1$. Keeping first two terms in the expansion, it was obtained in Ref.[14] that the correction

$$\Delta\alpha_B^{(1)}(r) = \frac{\pi^3}{6\beta_0[-\ln(\Lambda_V r)]^3}, \quad |\ln(\Lambda_V r)| \gg 1 \quad (50)$$

is positive and less than 5% only at very short distances, $r < 0.007$ fm. The important feature of $\Delta\alpha_B^{(1)}(r)$ is that it does not depend on the background mass m_B in limit $r \rightarrow 0$.

Secondly, the values of $\tilde{\alpha}_B^{(2)}(r)$ and $\alpha_s^{(2)}(r)$ coincide at the point $r = 0.041$ fm, i.e.

$$\Delta\alpha_B^{(2)}(r = 0.041 \text{ fm}) = 0 \quad (51)$$

At bigger distances, in particular, in the range

$$0.04 \text{ fm} < r \lesssim 0.15 \text{ fm} \quad (52)$$

this correction is negative and fast growing, e.g it is 13% at $r = 0.07$ fm, already 36% at $r = 0.10$ fm and reaches 100% at $r = 0.14$ fm although all these points lie rather far from the Landau pole, $r_{\text{pole}} = 0.29$ fm.

The explanation why the perturbative coupling is essentially larger than the background coupling at rather small r was given in Ref.[14]. It was shown there that in coordinate space the QCD constant Λ_R can be defined as a constant (given by Eq.(45)) only at very short distances while in the transition region (52) the role of QCD "constant" plays a function $\tilde{\Lambda}_R(r)$ dependent on the distance:

$$\Lambda_R \rightarrow \tilde{\Lambda}_R(r) \cong \Lambda_V \exp(\gamma_E + \sum_{k=1}^{\infty} \frac{(-m_B r)^k}{k!k}) \cong \Lambda_R \exp(-m_B r + \frac{1}{4}m_B^2 r^2) \quad (53)$$

Then with the use of the function $\tilde{\Lambda}_R(r)$ the perturbative coupling $\alpha_s^{(2)}(r)$ reproduces $\tilde{\alpha}_B^{(2)}(r)$ in the range (53) with the accuracy better than 5%. Actually, this approximation (54) can be used only at distances

$$m_B r - \frac{m_B^2 r^2}{4} < \gamma_E, \quad \text{or} \quad r \lesssim 0.15 \text{ fm}, \quad (54)$$

It is for this property of $\alpha_s^{(2)}(r)$ that we call in what follows the region (53) as the *transition region*.

At longer distances $\tilde{\Lambda}_R(r)$ is approaching the vector constant Λ_V :

$$\tilde{\Lambda}_R \rightarrow \Lambda_V \text{ at } r \gtrsim 0.15 \text{ fm} \quad (55)$$

In this region, as shown in Ref.[14], the background coupling can be approximated by two-loop expression $\alpha_B^{(2)}(q)$ in momentum space with the following prescription:

$$q \rightarrow \frac{1}{r}, \quad \Lambda = \Lambda_V; \quad (56)$$

or

$$\tilde{\alpha}_B^{(2)}(r) \approx \alpha_B^{(2)}(q = \frac{1}{r}) = \frac{4\pi}{\beta_0 t_R} \left\{ 1 - \frac{\beta_1}{\beta_0^2} \frac{\ln t_R}{t_R} \right\}, \quad (57)$$

where t_R depends on the background mass m_B ,

$$t_R = \ln \frac{1 + m_B^2 r^2}{\Lambda_V^2 r^2} \quad (58)$$

At $r \gtrsim 0.35$ fm the term $m_B^2 r^2$ under logarithm (58) is becoming dominant.

Thus one can conclude that the prescription of PQCD on the choice of the QCD constant in coordinate space as $\Lambda_R = \Lambda_V r^{\gamma_E}$ is valid only at very short distances, $r < 0.04$ fm. In the range $r \gtrsim 0.2$ fm, which is mostly important in hadron spectroscopy, $\tilde{\Lambda}_R \approx \Lambda_V$, i.e. about two times smaller than perturbative Λ_R . In the transition region (52) instead of the constant Λ_R the function $\tilde{\Lambda}_R(r)$ dependent on the distance should be introduced.

5 Static interquark potential

Knowing the differences $\Delta\alpha_B^{(n)}(r) \equiv \tilde{\alpha}_B^{(n)}(r) - \alpha_s^{(n)}(r)$ one can calculate the corresponding differences $\Delta V_B^{(n)}(r)$ between the background and perturbative static potentials:

$$\Delta V_B^{(n)}(r) = -\frac{4}{3} \frac{\Delta\alpha_B^{(n)}(r)}{r}, \quad (n = 1, 2). \quad (59)$$

Numerically calculated $\Delta V_B^{(1,2)}(r)$ are shown in Figs.5,6 correspondingly. We observe the linear rise of potentials illustrated by the tangents (dashed lines). Tangent slopes $\sigma_B^{(n)}(r)$ are defined as

$$\sigma_B^{*(n)}(r) = \frac{\partial \Delta V_B^{(n)}(r)}{\partial r}. \quad (60)$$

We see from the figures that

$$\sigma_B^{*(1)} = 1.20 \text{ GeV}^2, \quad 0.05 \text{ fm} < r < 0.12 \text{ fm}, \quad (61)$$

$$\sigma_B^{*(2)} = 0.87 \text{ GeV}^2, \quad 0.03 \text{ fm} < r < 0.09 \text{ fm}. \quad (62)$$

Such large potential difference originates for two reasons, first, it appears due to presence of the term $m_B^2 r^2$ under logarithm (58); second, $\tilde{\Lambda}_R(r)$ (54) (an analog of QCD constant) depends on r and fast decreasing in the transition region (52). This large difference means that the perturbative $\alpha_s(r)$ fails in this region. Nevertheless, we ought to compare our results (62),(63) with the lattice ones from Ref.[18]. After perturbative potential subtraction from

lattice static quenched potential, lattice data in the region $0.03 \text{ fm} < r < 0.15 \text{ fm}$ were parameterized by linear potential with the slope

$$\sigma_{\text{lat}}^* = (1.20 \pm 0.36) \text{ GeV}^2, \quad 0.03 \text{ fm} < r < 0.15 \text{ fm}. \quad (63)$$

One can see that σ_{lat}^* corresponds to $\sigma_B^{*(1,2)}$ within one standard error. We conclude that this too large linear slope of potential is well explained by using $\alpha_B(r)$ instead of $\alpha_s(r)$. In Fig.7 we describe lattice static potential from Ref.[18] at the distances $0.05 < r/r_0 < 0.45$ by the potential

$$V(r) = -\frac{4}{3} \frac{\alpha_B^{(2)}(r)}{r} + \sigma r + C, \quad (64)$$

where $\sigma = 0.2 \text{ GeV}^2$ and $C = -253 \text{ MeV}$ (shown by solid line). This potential includes background perturbative potential $V_B^{(2)}(r)$ and linear confining potential σr . Constant C corresponds to the quark self-energy. We observe that this potential remarkably describes all lattice data.

At the Fig.7 *1-loop* and *2-loop perturbative potentials*, calculated in Ref.[18], are also shown. The difference between them and lattice points is large and explained above. The *1-loop perturbative + linear potential* with the slope σ_{lat}^* is also shown. It describes lattice points up to $r/r_0 = 0.35$. It fails to describe the rest of data because of the Landau pole of $\alpha_s(r)$. On the contrary, $V(r)$ (Eq.(64)) not only describes all the presented in Fig.7 lattice data in the region $0.05 < r/r_0 < 0.3$, but also all lattice data available up to $r = 3r_0$ with a reasonable accuracy.

What is the physics of the linear part of $V(r)$? In the framework of BPTh it was shown in [27] that the linear confining potential arises starting from the quark distances around gluon correlation length T_g . From the lattice data $T_g \approx 0.2 \text{ fm}$ [28] or at least $T_g = 0.12 \div 0.15 \text{ fm}$ [29]. For this reason one needs to take into account an interference of perturbative and nonperturbative effects [30]. As was shown in Ref.[30], the interference potential at $r \lesssim T_g$ is close to linear with the slope about σ , while nonperturbative potential is proportional to r^2 and small in this region [27]. At distances $r \gtrsim T_g$, the interference interaction vanishes, while the NP potential becomes close to the linear one with the same slope σ . As a result the sum of these potentials may be close to linear all over the distances.

This linear behaviour of nonperturbative potential at short distances is also important for the fine structure fit in charmonium [10]. Note also that the linear potential $V^{(\text{NP})}(r)$ is consistent with the "short string" potential generated either by the topologically defined point-like monopoles or infinitely thin P-vortices within the Abelian Higgs model [31]. The distinguishing feature of last potential is that it does not change its slope at all distances. We leave the detailed numerical analysis of this effect to the subsequent paper.

6 Conclusions

In our paper the strong coupling $\tilde{\alpha}_B(r)$ in coordinate space, deduced in BPTh, is investigated and the corresponding perturbative potential is compared to short range lattice static potential from Ref. [18]. The following prominent features of $\tilde{\alpha}_B(r)$ are observed:

1. The background coupling goes over into standard perturbative coupling $\alpha_s(r)$ only at very short distances, $r < 0.04 \text{ fm}$, where the QCD constant $\Lambda_R = \Lambda_V \exp \gamma_E$ and Λ_V , the QCD constant in "vector scheme" is considered to be a well established number in quenched approximation.

2. At larger r a role of QCD constant plays a function $\tilde{\Lambda}_R(r)$ which at short distances, $m_B r < \gamma_E$, is approximately given by

$$\tilde{\Lambda}_R(r) \approx \Lambda_R \exp(-m_B r + \frac{m_B^2 r^2}{4}), \quad (65)$$

where $m_B = 1.0$ GeV is the background mass fixed by fit to fine structure splittings of $1P$ and $2P$ levels in bottomonium. In fact the condition

$$m_B r - \frac{1}{4} m_B^2 r^2 \leq \gamma_E \quad (66)$$

defines the narrow transition region: $0.05 \text{ fm} \leq r \leq 0.15 \text{ fm}$, where $\tilde{\Lambda}_R(r)$ decreases almost twice, from the value Λ_R at $r \approx 0.05 \text{ fm}$ to the number close to Λ_V at $r=0.15 \text{ fm}$.

3. The static potential $V_B(r)$ in BPTh, defined through $\tilde{\alpha}_B(r)$ in usual way, appears to be in a good agreement with quenched lattice static potential measured at short distances [18].

4. The specific behavior of $\tilde{\alpha}_B(r)$ in the transition region produces linear rise of the difference $\Delta V(r) = V_B(r) - V_P(r)$ with the slope $\sigma^* \sim 1 \text{ GeV}^2$ in accord to lattice data. Moreover, we have obtained a very good agreement with the lattice data using the sum $V_B(r) + \sigma r$ with $\sigma = 0.2 \text{ GeV}^2$.

5. At distances $r \gtrsim 0.2 \text{ fm}$ the function $\tilde{\Lambda}_R(r)$ turns out to be almost constant; $\tilde{\Lambda}_R(r) \approx \Lambda_V$ over all distances, so that at $r > 0.3 \text{ fm}$ the coupling $\tilde{\alpha}_B(r)$ fast approaches the freezing value $\tilde{\alpha}_B(\infty)$. This fact helps to understand why the use of $\alpha_s(r)=\text{const}$ in static potential appears to be a good approximation in hadron spectroscopy.

6. The freezing value of the background coupling coincides in momentum and coordinate space and this statement can be checked in different processes in low energy QCD. Our estimate for α_{fr} is 0.53-0.60.

The authors are grateful to Yu.A.Simonov for many fruitful discussions. This work has been supported by RFFI grant 00-02-17836.

References

- [1] E.Eichten et.al., Phys. Rev. Lett. **34**, 369 (1975); Phys. Rev. **D21**, 203 (1980)
- [2] L.Richardson, Phys. Lett. **B82**, 272 (1979)
- [3] S.Godfrey and N.Isgur, Phys. Rev, **D32**, 189 (1985)
- [4] A.C.Mattingly and P.M.Stevenson, Phys. Rev **D49**, 437 (1994)
- [5] A.M.Badalian, Phys. Atom. Nucl. **60**, 1003 (1997); translated from Yad.Fiz. **60**, 1122 (1997); hep-lat/9704004
- [6] Yu. L.Dokshitzer, V.A.Khose, and S.I.Troyan, Phys. Rev. **D53**, 89 (1996); Yu. L.Dokshitzer, hep-ph/9812252
- [7] Yu.A.Simonov, Perturbative QCD in the nonperturbative QCD vacuum, Proc of Schlading Winter School, March 1996, Springer, v.479, p. 139 (1997); Pis'ma Zh. Eks. Theor. Fiz. **57**, 513 (1993); Yad. Fiz. **58**, 113 (1995)

- [8] A.M.Badalian and Yu.A.Simonov, Phys. Atom Nucl. **60** 630 (1997), translated from Yad. Fiz. **60**, 714 (1997)
- [9] D.V.Shirkov and I.L.Solovtsov, phys. Rev. Lett. **79**, 1209 (1997);
D.V.Shirkov Nucl. Phys. B (proc. Suppl.) **64** 106 (1998)
- [10] A.M.Badalian and V.L.Morgunov, Phys. Rev. **D60** 116008 (1999), hep-ph/9901430;
Phys. Atom Nucl. **62**, 1019 (1999) translated from Yad. Fiz. **62**, 1086 (1999)
- [11] A.M.Badalian and B.L.G.Bakker, Phys. Rev. **D62**, 094031 (2000); hep-ph/0004021
- [12] Yu.S.Kalashnikova, A.V.Nefediev, and Yu.A.Simonov, hep-ph/0103274, Phys. Rev. D,
to be published.
- [13] M.Jezabek, M.Peter, and Y.Sumino, Phys. Lett. **B428**, 352 (1998), hep-ph/9803337
- [14] A.M.Badalian, Phys. Atom. Nucl. **63**, 2173 (2000) (translated from Yad Fiz.) **63**, 2269
(2000)
- [15] S.P.Booth et.al. Phys. Lett. **B294**, 385 (1992); K.D.Born, E.Laermann, T.F.Walsh, and
P.M.Zerwas, Phys. Lett. **B329** ; 325 (1994)
- [16] G.S.Bali and K.Schilling, Phys. Rev. **D47**, 661 (1993); G.S.Bali, K.Schilling, and
A.Wachter, Phys. Rev. **D56** 2566 (1997)
- [17] SESAM collaboration, U.Glässner et.al. Phys. Lett. **B383**, 98 (1996), hep-lat/0002028;
C.Bernard et.al., Phys. Rev. **D62**, 034503 (2000)
- [18] G.S.Bali, Phys. Lett. **B460**, 170 (1999)
- [19] S.Capitani, M.Lüscher, R.Sommer and H.Witting, Nucl. Phys. **B544**, 669 (1999)
- [20] M.Peter, Phys. Rev. Lett. **78** 602 (1997); Nucl. Phys. **B501**, 471 (1997)
- [21] Y.Schröder, Phys. Zett. **B447**, 321 (1999)
- [22] Yu.A.Simonov, Yad.Fiz. **58**, 113 (1995)
- [23] G.Parisi and R.Petronzio, Phys. Lett. **B94**, 51 (1980);
J.M.Cornwall, Ph.Rev. **D26**, 1453 (1982)
- [24] A.Billoire, Phys. Lett. **B92**, 343 (1980)
- [25] Particle Data Group, Eur. Phys. Journ. C, **15**, 85 (2000)
- [26] F.J.Yndurain, hep-ph/9910399
- [27] Yu.A.Simonov, Nucl. Phys. **B307**, 512 (1988);
A.M.Badalian and V.P.Yurov, Phys. Atom. Nucl. **56**, 176 (1993)(translated from Yad.
Fiz.) **56**, 239 (1993);
A.M.Badalian and Yu.A.Simonov, Phys. Atom Nucl. **59**, 2164 (1996), (translated from
Yad. Fiz.) **59**, 2247 (1996)
- [28] A.Di.Giacomo and H.Panagopoulos, Phys. Lett. **B285**, 133 (1999)

- [29] G.Bali, N.Bramilla, and A.Vairo, Phys. Lett. **B421**, 265 (1998); hep-lat/9709079
- [30] Yu.A.Simonov, Phys.Rept. 320, 265 (1999)
- [31] V.I.Zakharov, Lecture given at the Winter School of physics of ITEP, February 1999;
M.N.Chernodub, F.V.Gubarev, M.V.Polikarpov, and V.I.Zakharov, Phys.Lett. **B475**,
303 (2000).

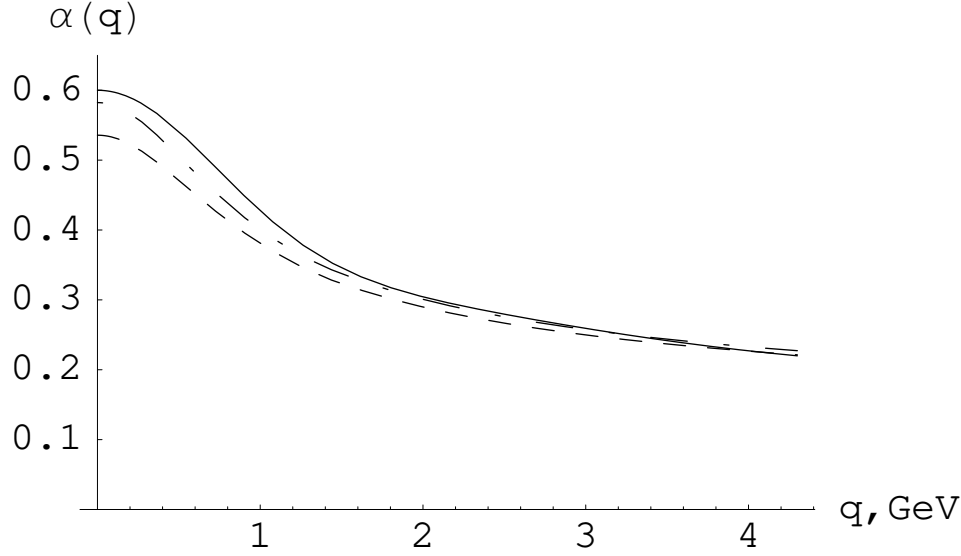


Figure 1: The behavior of the background coupling $\alpha_B^{(2)}(q)$ for $\Lambda_V^{(3)} = 385$ MeV (dashed line) and for $\Lambda_V^{(3)} = 410$ MeV (dash-dotted line) compared to the phenomenological coupling $\alpha_{\text{GI}}(q)$ (solid line) taken from Ref.[3].

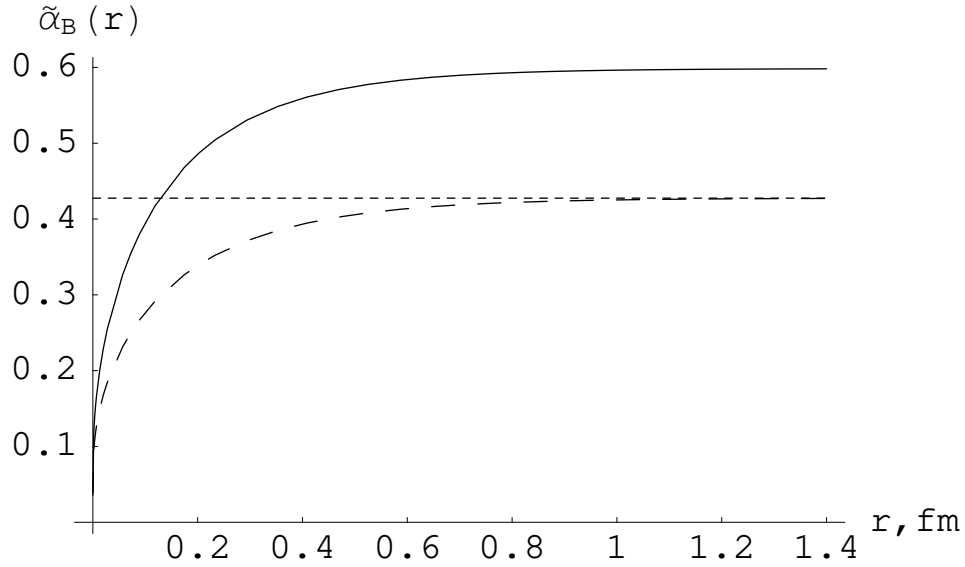


Figure 2: The 1-loop $\tilde{\alpha}_B^{(1)}(r)$ (solid line) and the 2-loop $\tilde{\alpha}_B^{(2)}(r)$ (dashed line) background couplings in quenched approximation; in both cases $\Lambda_V^{(0)} = 385$ MeV, $m_B = 1.0$ GeV; 2-loop asymptotics, $\alpha_{\text{cr}}^{(2)} = 0.428$, is shown.

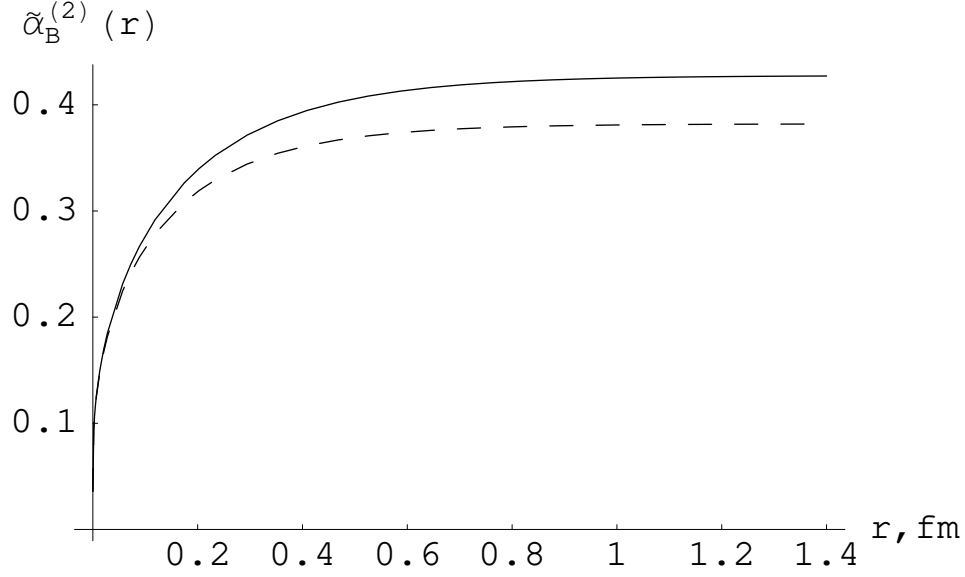


Figure 3: The background coupling $\tilde{\alpha}_B^{(2)}(r)$ in coordinate space for two values of the background mass m_B : $m_B = 1.0$ GeV (solid line) and $m_B = 1.1$ GeV (dashed line); in both cases $\Lambda_V^{(0)} = 385$ MeV.

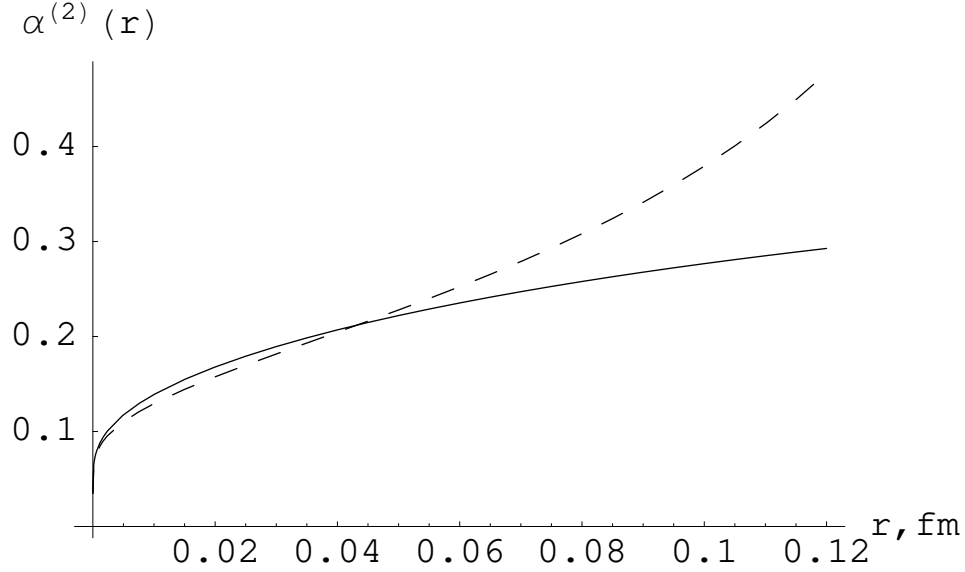


Figure 4: The background coupling $\tilde{\alpha}_B^{(2)}(r)$ with $\Lambda_V^{(0)} = 385$ MeV, $m_B = 1.0$ GeV (solid line) compared to the perturbative $\alpha_s^{(2)}(r)$ with $\Lambda_R = 686$ MeV (dashed line) at short distances.

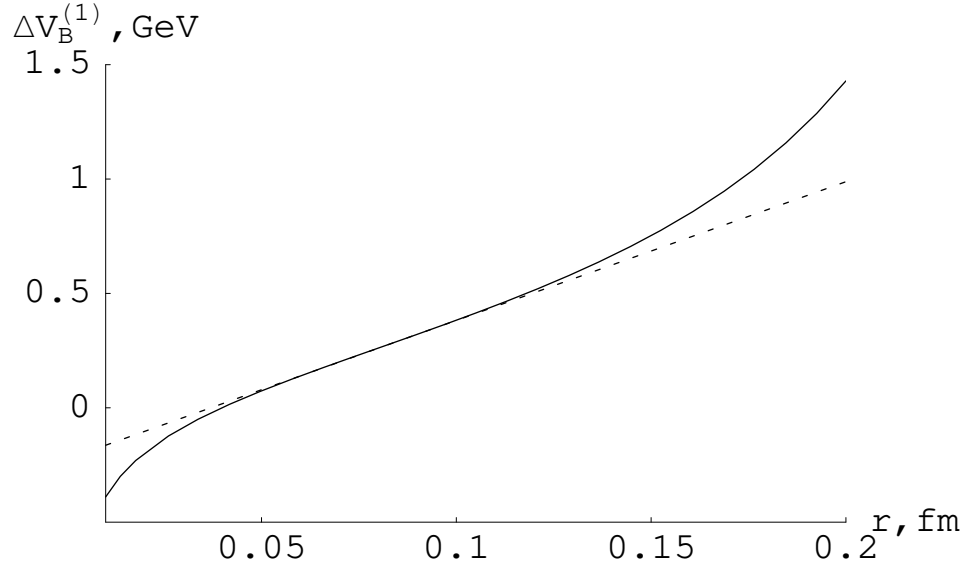


Figure 5: The difference $\Delta V_B^{(1)}$ of the background and perturbative potentials in one-loop approximation (solid line). The tangent with the slope $\sigma_B^{*(1)} = 1.20 \text{ GeV}^2$ is shown by dashed line. The parameters are the same as in Fig. 4.

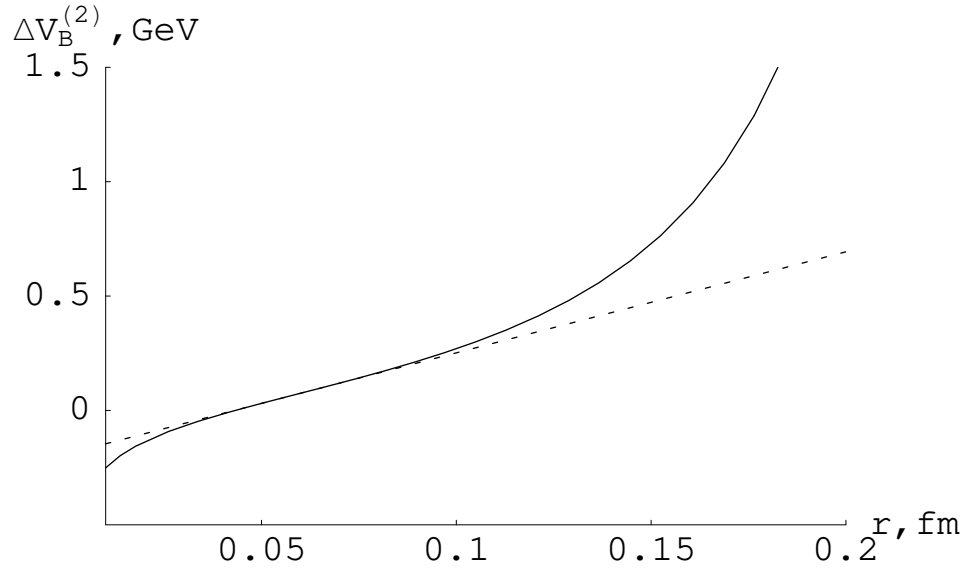


Figure 6: The difference $\Delta V_B^{(2)}$ of the background and perturbative potentials in two-loop approximation (solid line). The tangent with the slope $\sigma_B^{*(2)} = 0.87 \text{ GeV}^2$ is shown by dashed line. The parameters are the same as in Fig. 4.

This figure "Figure7.gif" is available in "gif" format from:

<http://arxiv.org/ps/hep-ph/0104097v1>